

Chapter 11

Parametric Amplifiers and Oscillator

A device exhibiting a negative conductance, such as a tunnel diode, can be utilized to construct an amplifier and oscillator. A laser is also categorized as a negative conductance oscillator as we have seen in the previous chapter. There is another class of amplifier and oscillator, which is based on non-linear susceptances and known as a parametric amplifier/oscillator.

For instance, a reverse-biased pn junction has the non-linear charge-voltage characteristic due to the voltage-dependent capacitance. The mixing occurs between the three frequency components of signal, idler and pump waves in such a nonlinear element and the energy flows from a strong pump wave to weak signal and idler waves. This flow of the power from the pump to the signal introduces the negative conductance into the signal circuit. In optical spectral domain, the atomic dipole moment, driven by an intense pump laser, features a similar non-linearity and is capable of amplifying weak signal and idler waves.

11.1 Non-Degenerate Parametric Amplifier

11.1.1 Principle of Operation

An equivalent circuit for a non-degenerate parametric amplifier is shown in Fig. 11.1. A nonlinear capacitor is surrounded by three parallel LCR circuits, which represent the signal, idler and pump circuits, respectively.

The charge q on the nonlinear capacitance is a function of the voltage across its terminals. Using the Taylor series expansion, the charge may be expressed in the form:

$$q(t) = a_1v(t) + a_2v^2(t) + a_3v^3(t) + \dots \quad (11.1)$$

When all the coefficients except the first and second terms are zero, the charge varies quadratically with the voltage,

$$q(t) = Cv(t) + a_2v^2(t) \quad , \quad (11.2)$$

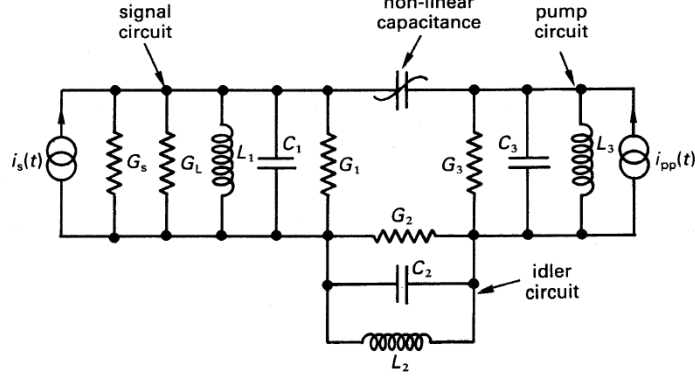


Figure 11.1: An equivalent circuit of a non-degenerate parametric amplifier.

where a_1 is just replaced by the linear capacitance C . The current flowing in the nonlinear capacitance is

$$i(t) = \frac{dq(t)}{dt} = C \frac{dv(t)}{dt} + 2a_2 v(t) \frac{dv(t)}{dt} \quad , \quad (11.3)$$

where the voltage across the nonlinear capacitance consists of the signal, idler and pump waves at angular frequencies ω_1 , ω_2 , and ω_3 , respectively,

$$\begin{aligned} v(t) &= v_1(t) + v_2(t) + v_3(t) \\ &= V_1 \cos(\omega_1 t + \phi_1) + V_2 \cos(\omega_2 t + \phi_2) + V_3 \cos(\omega_3 t + \phi_3) \quad . \end{aligned} \quad (11.4)$$

The angular frequencies in Eq. (11.4) satisfy

$$\omega_3 = \omega_1 + \omega_2 \quad , \quad (11.5)$$

$$\omega_i = 1/\sqrt{L_i(C_i + C)} \quad . \quad (11.6)$$

Using Eq. (11.4) in Eq. (11.3), we obtain the expression for the current,

$$i(t) = i_1(t) + i_2(t) + i_3(t) \quad , \quad (11.7)$$

where

$$i_1(t) = -\omega_1 C V_1 \sin(\omega_1 t + \phi_1) - \omega_1 a_2 V_2 V_3 \sin(\omega_1 t + \phi_3 - \phi_2) \quad , \quad (11.8)$$

$$i_2(t) = -\omega_2 C V_2 \sin(\omega_2 t + \phi_2) - \omega_2 a_2 V_1 V_3 \sin(\omega_2 t + \phi_3 - \phi_1) \quad , \quad (11.9)$$

$$i_3(t) = -\omega_3 C V_3 \sin(\omega_3 t + \phi_3) - \omega_3 a_2 V_1 V_2 \sin(\omega_3 t + \phi_1 + \phi_2) \quad . \quad (11.10)$$

Equations (11.8)-(11.10) can be rewritten as

$$i_1(t) = C \frac{dv_1(t)}{dt} + \frac{a_2 V_2 V_3}{V_1} \left\{ \cos(\phi_3 - \phi_2 - \phi_1) \frac{dv_1(t)}{dt} - \omega_1 v_1(t) \sin(\phi_3 - \phi_2 - \phi_1) \right\} \quad , \quad (11.11)$$

$$i_2(t) = C \frac{dv_2(t)}{dt} + \frac{a_2 V_1 V_3}{V_2} \left\{ \cos(\phi_3 - \phi_2 - \phi_1) \frac{dv_2(t)}{dt} - \omega_2 v_2(t) \sin(\phi_3 - \phi_2 - \phi_1) \right\} , \quad (11.12)$$

$$i_3(t) = C \frac{dv_3(t)}{dt} + \frac{a_2 V_1 V_2}{V_3} \left\{ \cos(\phi_3 - \phi_2 - \phi_1) \frac{dv_3(t)}{dt} + \omega_3 v_3(t) \sin(\phi_3 - \phi_2 - \phi_1) \right\} . \quad (11.13)$$

Taking the Fourier transform of Eqs. (11.11)-(11.13), we obtain the admittances Y_i ($i = 1, 2, 3$) seen by the signal, idler and pump circuits:

$$Y_1 = \frac{I_1(j\omega)}{V_1(j\omega)} = j\omega_1 C + j\omega_1 a_2 \frac{V_2 V_3}{V_1} \exp[j(\phi_3 - \phi_2 - \phi_1)] , \quad (11.14)$$

$$Y_2 = \frac{I_2(j\omega)}{V_2(j\omega)} = j\omega_2 C + j\omega_2 a_2 \frac{V_1 V_3}{V_2} \exp[j(\phi_3 - \phi_2 - \phi_1)] , \quad (11.15)$$

$$Y_3 = \frac{I_3(j\omega)}{V_3(j\omega)} = j\omega_3 C + j\omega_3 a_2 \frac{V_1 V_2}{V_3} \exp[-j(\phi_3 - \phi_2 - \phi_1)] . \quad (11.16)$$

The current-voltage relations for the three circuits are given by

$$I_s(j\omega) = \left\{ G_T + j\omega_1 a_2 \frac{V_2 V_3}{V_1} \exp[j(\phi_3 - \phi_2 - \phi_1)] \right\} V_1(j\omega) , \quad (11.17)$$

$$O = \left\{ G_2 + j\omega_2 a_2 \frac{V_1 V_3}{V_2} \exp[j(\phi_3 - \phi_2 - \phi_1)] \right\} V_2(j\omega) , \quad (11.18)$$

$$I_P(j\omega) = \left\{ G_3 + j\omega_3 a_2 \frac{V_1 V_2}{V_3} \exp[-j(\phi_3 - \phi_2 - \phi_1)] \right\} V_3(j\omega) . \quad (11.19)$$

Here $I_s(j\omega)$ and $I_P(j\omega)$ are the Fourier transforms of the input signal and pump currents, respectively, and $G_T = G_s + G_L + G_1$. The LC circuit resonant condition Eq. (11.6) is used.

By eliminating V_2 and V_3 from Eq. (11.17) using Eqs. (11.18) and (11.19), we obtain the admittance of the signal circuit,

$$Y_s = G_T - G = G_T - \frac{\omega_1 \omega_2 a_2^2}{G_2 G_3^2} \frac{|I_P(j\omega)|^2}{\left[1 + \frac{\omega_2 \omega_3}{G_2 G_3} a_2^2 V_1^2\right]^2} . \quad (11.20)$$

There emerges a negative conductance due to the nonlinear capacitance driven by the pump wave at ω_3 . If V_1 satisfies the condition,

$$\frac{\omega_2 \omega_3}{G_2 G_3} a_2^2 V_1^2 \ll 1 , \quad (11.21)$$

the negative conductance is independent of the signal input and the linear parametric amplification is realized.

11.1.2 Power Gain

The power gain G of the non-degenerate parametric amplifier is given by the ratio of the power delivered to the load G_L to the input power to the source G_s :

$$\begin{aligned} G &= \frac{G_L V_1^2}{(|I_s|^2/4G_s)} \\ &= \frac{4G_s G_L}{|Y_s|^2} . \end{aligned} \quad (11.22)$$

When there is no pump ($|I_P(j\omega)| = 0$), the amplifier has no gain ($Y_s = G_T$). When the pump current reaches the threshold:

$$|I_P(j\omega)|^2 = \frac{G_T G_2 G_3^2}{\omega_1 \omega_2 a_2^2} , \quad (11.23)$$

the system becomes unstable ($|Y_s| \rightarrow 0$) and the amplifier starts to oscillate. Between these two extreme conditions, linear amplification of the input signal is provided as far as the signal is not too strong, i.e. Eq. (11.21) is satisfied.

11.1.3 Noise Figure

The noise in a parametric amplifier is generated by the circuit conductance G_s, G_1 and G_2 . The noise generated by the pump circuit conductance G_3 can be normally neglected because the pump current $i_P(t)$ is usually very large and well approximated as a noise-free sinusoidal wave. The noise from the load conductance G_L is ignored, because it is usually taken into account in the following state.

Equation (11.17) suggests that a voltage fluctuation ΔV_2 across the idler circuit at frequency ω_2 results in a current fluctuation ΔI_s in the signal circuit at frequency ω_1 . The spectral density of the voltage fluctuation ΔV_2 is given by

$$\overline{S_{V_2}(\omega)} = \begin{cases} 4k_B T / G_2 & \text{(thermal limit)} \\ 2\hbar\omega_2 / G_2 & \text{(quantum limit)} \end{cases} . \quad (11.24)$$

The spectral density of the induced current fluctuation ΔI_s is given by

$$\overline{S_{I_{s2}}(\omega)} = \omega_1^2 |C'|^2 \overline{S_{V_2}(\omega)} , \quad (11.25)$$

where

$$|C'| = a_2 V_3 \simeq a_2 |I_P(j\omega)| / G_3 . \quad (11.26)$$

The second equality is obtained by neglecting the gain saturation effect Eq. (11.21).

The spectral densities of the current generators associated with G_s and G_1 are

$$\overline{S_{I_{ss}}(\omega)} = \begin{cases} 4k_B T G_s \\ 2\hbar\omega_1 G_s \end{cases} , \quad (11.27)$$

$$\overline{S_{I_{s1}}(\omega)} = \begin{cases} 4k_B T G_1 \\ 2\hbar\omega_1 G_1 \end{cases} . \quad (11.28)$$

Since there is no correlation between these three noise sources, the noise figure of the amplifier in the thermal limit can be written as

$$\begin{aligned} F &= \frac{\overline{S_{I_{ss}}(\omega)} + \overline{S_{I_{s1}}(\omega)} + \overline{S_{I_{s2}}(\omega)}}{\overline{S_{I_{ss}}(\omega)}} \\ &= 1 + \frac{G_1}{G_s} + \frac{\omega_1^2 |C'|^2}{G_2 G_s} \quad . \end{aligned} \quad (11.29)$$

From Eqs. (11.20) and (11.26), we can express $|C'|^2$ in terms of the negative conductance G ,

$$|C'|^2 = \frac{G_2 G}{\omega_1 \omega_2} \quad . \quad (11.30)$$

Using Eq. (11.30) in Eq. (11.29), the noise figure is expressed as

$$F = 1 + \frac{G_1}{G_s} + \frac{\omega_1}{\omega_2} \frac{G}{G_s} \quad . \quad (11.31)$$

The noise figure can be reduced to one (ideal amplification) by achieving the negligible internal loss in the signal circuit ($G_1 \ll G_s$) and the large ratio of $\omega_1/\omega_2 \ll 1$.

The noise figure of the amplifier in the quantum limit is, on the other hand, given by

$$F = 1 + \frac{G_1}{G_s} + \frac{G}{G_s} \quad . \quad (11.32)$$

In a high gain amplifier $G \simeq G_s (G_1, G_L \ll G_s)$ at the quantum limit, the minimum noise figure is $F_{min} = 2(3 \text{ dB})$ instead of $F_{min} = 1(0 \text{ dB})$ at the thermal limit.

11.2 Degenerate Parametric Amplifier

11.2.1 Principle of Operation

When the signal and idler waves have identical frequencies, such a parametric amplifier is called a degenerate parametric amplifier and has a unique characteristic. Consider a swing driven by a person (Fig. 11.2(a)). During one-half cycle (left to right) of the swing, the person makes a full one cycle (up-down-up). The frequency of the driving person (pump) and that of the driven swing (signal) satisfy $\omega_P = 2\omega_s$. Figure 11.2(b) is an equivalent LCR circuit of the swing, in which the driving action of the person is represented by the nonlinear capacitor.

The circuit equations are given by

$$\begin{aligned} -I &= \frac{d}{dt}Q = \frac{d}{dt}CV \\ V &= RI + L \frac{d}{dt}I \end{aligned} \quad (11.33)$$

Eliminating the current I from Eq. (11.33), we obtain

$$\left[\frac{d^2}{dt^2} + \frac{R}{L} \frac{d}{dt} + \frac{1}{LC} \right] V = 0 \quad (11.34)$$

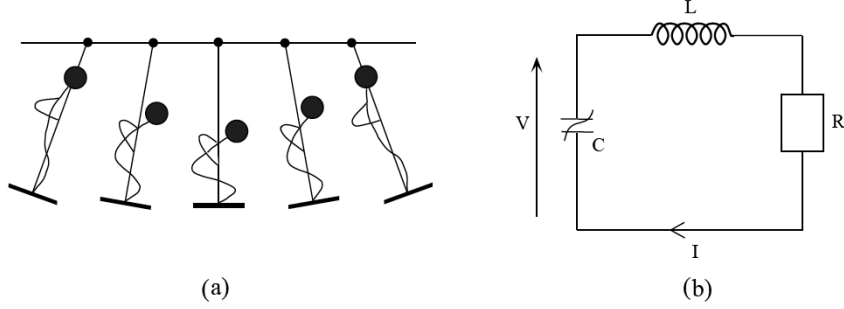


Figure 11.2: A swing driven by a person and an equivalent circuit.

The solution of a damped harmonic oscillator expressed by Eq. (11.34) is

$$V = V_0 \exp\left(-\frac{Rt}{2L}\right) \exp\left(\pm j\sqrt{\omega_0^2 - \frac{R^2}{4L^2}}t\right) . \quad (11.35)$$

If the capacitance is modulated at the pump frequency ω_P as

$$C = C_0 [1 - \Delta C \sin(\omega_P t + \phi)] , \quad (11.36)$$

Equation (11.34) is modified to

$$\left\{ \frac{d}{dt^2} + \frac{R}{L} \frac{d}{dt} + \omega_0^2 \left[1 + \frac{\Delta C}{C_0} \sin(\omega_P t + \phi) \right] \right\} V \simeq 0 , \quad (11.37)$$

where $\omega_0 = 1/\sqrt{LC_0}$ and it is assumed $\Delta C \ll C_0$. If we assume the solution of Eq. (11.37) has the form,

$$V = \text{Re} \{ 2V_0 \exp(\alpha t) \exp(j\omega t) \} , \quad (11.38)$$

we obtain

$$\begin{aligned} 2V_0 \exp(\alpha t) & \left[\left(\alpha^2 - \omega^2 + \frac{R}{L} \alpha + \omega_0^2 \right) \cos(\omega t) - \left(2\omega \alpha + \frac{R}{L} \omega \right) \sin(\omega t) \right] \\ & = -2V_0 \exp(\alpha t) \frac{\omega_0^2 \Delta C}{2C_0} [\sin \omega t \cos \phi + \cos \omega t \sin \phi] . \end{aligned} \quad (11.39)$$

By comparing the $\cos \omega t$ and $\sin \omega t$ terms in both sides of Eq. (11.39), we have the equations which determine the new oscillation frequency ω and amplification/attenuation coefficient α :

$$\omega^2 = \omega_0^2 + \alpha^2 + \frac{R}{L} \alpha + \frac{\omega_0^2 \Delta C}{2C_0} \sin \phi , \quad (11.40)$$

$$2\alpha = \frac{\omega_0 \Delta C}{2C_0} \cos \phi - \frac{R}{L} . \quad (11.41)$$

If $\phi = 0$ and $\Delta C > \frac{2RC_0}{\omega_0 L}$, we have a growing solution ($\alpha > 0$). The energy is provided to the signal from the pump. If $\phi = \frac{\pi}{2}$ or $\frac{3\pi}{2}$, there is no energy exchange between the pump and signal waves. If $\phi = \pi$, we have an attenuating solution ($\alpha < -\frac{R}{L}$). The energy is extracted from the signal and transferred to the pump.

11.2.2 Phase Sensitive Amplifier

Changing the pump phase from $\phi = 0$ to $\phi = \pi$ in Eq. (11.36) corresponds to shifting the capacitance modulation by half a pump period, which is equivalent to one-quarter signal period. That is, one quadrature amplitude of the signal wave corresponding to the $\phi = 0$ solution is amplified by a gain coefficient $2\alpha = \frac{\omega_0 \Delta C}{2C_0} - \frac{R}{L}$ but the other quadrature amplitude corresponding to the $\phi = \pi$ solution is deamplified by an attenuation coefficient $2\alpha' = -\frac{\omega_0 \Delta C}{2C_0} - \frac{R}{L}$. This type of operation is called a phase sensitive amplifier. If the signal wave is expressed by the two quadrature amplitudes a_1 and a_2 as

$$E_s = a_1 \cos \omega_s t + a_2 \sin \omega_s t \quad , \quad (11.42)$$

and the pump phase is set to amplify the $\cos \omega_s t$ component and deamplify the $\sin \omega_s t$ component, the two-kinds of input signals with isotropic (phase insensitive) noise are transformed to the squeezed state as shown in Fig. 11.3. When the input noise is dominated by thermal noise, the process is called thermal noise squeezing or classical squeezing. When the input noise is dominated by quantum mechanical zero-point noise, the process is called quantum noise squeezing.

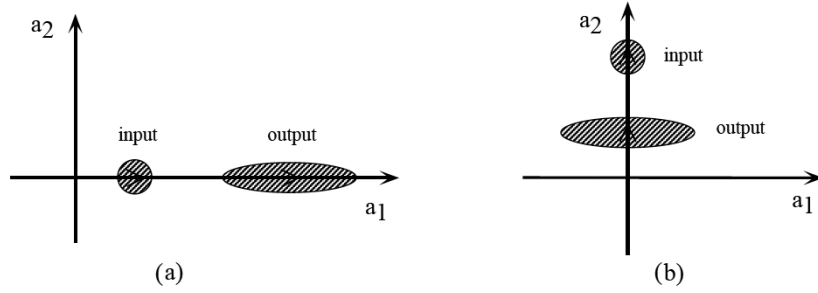


Figure 11.3: The input and output signals of a degenerate parametric amplifier.

11.3 Quantum Limit of a Linear Amplifier

The simplified input-output relations for a degenerate parametric amplifier are given by

$$b_{s1} = \sqrt{G} a_{s1} \quad , \quad (11.43)$$

$$b_{s2} = \frac{1}{\sqrt{G}} a_{s2} \quad , \quad (11.44)$$

where $a_{s1}(b_{s1})$ and $a_{s2}(b_{s2})$ are the $\cos \omega_s t$ and $\sin \omega_s t$ components of the input (output) signal waves. Equation (11.43) indicates that the amplification of one quadrature component does not introduce any additional noise. The noise figure of this amplifier is

$$F = \frac{\langle \Delta b_{s1}^2 \rangle}{G \langle \Delta a_{s1}^2 \rangle} = 1 \quad (0\text{dB}) \quad . \quad (11.45)$$

The sacrifice of the noise-free amplification is the loss of the signal information stored in the other quadrature a_{s2} since that quadrature component is deamplified.

The input-output relations for a nondegenerate parametric amplifier are given by

$$b_{s1} = \sqrt{G}a_{s1} + \sqrt{G-1}a_{i1} \quad , \quad (11.46)$$

$$b_{s2} = \sqrt{G}a_{s2} - \sqrt{G-1}a_{i2} \quad , \quad (11.47)$$

where a_{i1} and a_{i2} are the $\cos \omega_i t$ and $\sin \omega_i t$ components of the input idler wave. The nondegenerate parametric amplifier allows the extraction of the two quadrature information simultaneously, but the amplifier introduces the additional noise. The minimum noise figure in this case is

$$F = \frac{\langle \Delta b_{s1}^2 \rangle}{G \langle \Delta a_{s1}^2 \rangle} = 2 \quad (3 \text{ dB}) \quad , \quad (11.48)$$

where it is assumed that the signal and idler carries the identical noise, i.e. $\langle \Delta a_{s1}^2 \rangle = \langle \Delta a_{i1}^2 \rangle$. This typical situation corresponds to the case that the input signal wave is in a coherent state and the input idler wave is in a vacuum state (no input), where $\langle \Delta a_{s1}^2 \rangle = \langle \Delta a_{i1}^2 \rangle = \frac{1}{4}$.

A microwave nondegenerate parametric amplifier is dominated by thermal noise rather than quantum noise. In such a case, cooling the idler input port to below the noise equivalent temperature of the signal channel is effective to reduce the noise figure. Indeed, the noise figure of close to 0 dB is achieved in a microwave nondegenerate parametric amplifier by this technique.

11.4 Quantum Correlation between Signal and Idler Waves from Nondegenerate Parametric Amplifiers

See "Phys. Rev. A38, 3556 (1988)".

Bibliography

- [1] A. von der Ziel, J. Appl. Phys. **19**, 999 (1948).
- [2] J. M. Manley and H. E. Rowe, Proc. IRE **47**, 2115 (1959).
- [3] M. Uenohara, Low Noise Amplification, Handbuch der Physik, vol. 23 (Springer, Berlin, 1962).
- [4] J. A. Giordmaine and R. C. Miller, Phys. Rev. Lett. **14**, 973 (1965).
- [5] S. E. Harris, M. K. Oshman and R. L. Byer, Phys. Rev. Lett. **18**, 732 (1967).
- [6] H. A. Haus and J. A. Mullen, Phys. Rev. **128**, 2407 (1962).
- [7] C. M. Caves, Phys. Rev. **D23**, 1693 (1981).

Quantum correlation and state reduction of photon twins produced by a parametric amplifier

K. Watanabe and Y. Yamamoto

Nippon Telephone and Telegraph Corporation Basic Research Laboratories, Musashino-shi, Tokyo 180, Japan

(Received 18 March 1988)

Signal and idler waves produced by a nondegenerate parametric amplifier feature strong positive correlation between their photon numbers, or in-phase amplitudes. They feature equally strong negative correlation between their phases, or quadrature-phase amplitudes. These photon twins can produce arbitrarily squeezed states via state reduction by appropriate measurements of an idler wave. When the quadrature amplitude of an idler wave is measured, the signal wave is collapsed to a quadrature-amplitude squeezed state. When the two-quadrature amplitudes of an idler wave are measured simultaneously, the signal wave becomes a coherent state.

I. INTRODUCTION

Nonclassical light is usually generated by one of two schemes. The first is a phase-sensitive amplification-deamplification in a four-wave mixer¹ or a degenerate parametric amplifier.² The second is amplitude saturation and phase diffusion in a pump-noise-suppressed laser.³ This paper discusses a completely different approach using nonunitarity state reduction by quantum measurement.

Arthurs and Kelly demonstrated that the system wave function can be reduced to a new state after the simultaneous measurement of two conjugate observables. This reduction realizes the arbitrary distribution of quantum noise determined by the measurement resolution of the two observables.⁴ However, these authors have not shown any physically realizable Hamiltonian for such measurement. At optical frequencies, the photon number \hat{n} , the quadrature amplitude \hat{a}_1 , and the two-quadrature amplitudes \hat{a}_1 and \hat{a}_2 are physically measured by a photon counter, homodyne detector, and heterodyne detector, respectively.⁵ Von Neumann's projection postulate has been generalized to characterize these measurements quantum mechanically.^{6,7} The generalized projectors, or operation-valued measures for these measurements, are given by $|n\rangle\langle n|$, $|\alpha_1\rangle\langle\alpha_1|$, and $|\alpha\rangle\langle\alpha|$. However, the measurements themselves are not considered as processes for generating number states $|n\rangle$, quadrature-amplitude eigenstates $|\alpha_1\rangle$, and coherent states $|\alpha\rangle$, because the electromagnetic fields are completely absorbed after these measurements are made.

To produce quantum light via state reduction by quantum measurement, quantum correlation between a signal and probe waves must first be established. Destructive measurement can be then performed on the probe wave. An example is the quantum nondemolition measurement of photon number, in which the signal waves is collapsed into a number-phase squeezed state after the signal photon number is nondestructively measured via destructive measurement of the probe phase.⁸

When a signal and idler waves are amplified in a non-

degenerate parametric amplifier, the outputs are correlated both in photon number and phase.⁹⁻¹¹ Measurement of the idler output wave provides information on the signal output. This suggests the generation of quantum light is possible via nonlinear parametric amplification of idler and signal waves, and subsequent measurement of the idler output.

This paper is organized as follows. In Sec. II we briefly review the evolution of a combined signal-and-idler density operator in a nondegenerate parametric amplifier. The reduced density operator of a signal wave is discussed, which corresponds to the signal quantum state without measurement. State reduction resulting from measurement of idler quadrature amplitude is treated in Sec. III. State reduction resulting from simultaneous measurement of the two idler quadrature amplitudes is studied in Sec. IV. A projection operator that maps a coherent state onto a number-phase squeezed state, quadrature-amplitude squeezed state, and coherent state is derived in Sec. V using the results of Secs. III and IV. In Sec. VI feedforward manipulation of a signal wave according to the measurement results to continuously generate nonclassical light with a fixed eigenvalue is determined. Finally, in Sec. VII, quantum correlations of signal and idler waves are studied using a Heisenberg picture. We present a physical interpretation of the results in Secs. III and IV.

II. STATE EVOLUTION IN A NONDEGENERATE PARAMETRIC AMPLIFIER

In this section we briefly review the evolution operator \hat{U} and the density operator $\hat{\rho}_{si}$ for signal and idler waves for the nondegenerate parametric amplifier.¹² The interaction Hamiltonian is

$$\hat{H}_{\text{int}} = \hbar[\kappa\hat{a}_s^\dagger\hat{a}_i^\dagger + \kappa^*\hat{a}_s\hat{a}_i], \quad (1)$$

and thus the differential equation for \hat{U} is

$$\frac{d\hat{U}}{dt} = -i\kappa_0[e^{i\theta}\hat{a}_s^\dagger\hat{a}_i^\dagger + e^{-i\theta}\hat{a}_s\hat{a}_i]\hat{U}, \quad (2)$$

where $\kappa = \kappa_0 e^{i\theta}$, κ_0 is a real constant, κ is a parametric interaction coefficient, and \hat{a}_s and \hat{a}_i are signal and idler annihilation operators.

From Refs. 12 and 13, we obtain the evolution opera-

tor, the output density operator with number state $|n_0\rangle$ as the input-signal state and the output density operator with coherent state $|\alpha_0\rangle$ as the input-signal state:

$$\hat{U} = \exp[-\ln \cosh(\kappa_0 t)] \exp[-ie^{i\theta} \tanh(\kappa_0 t) \hat{a}^\dagger \hat{a}_s^\dagger] \exp\{-\ln[\cosh(\kappa_0 t) \hat{a}^\dagger \hat{a}_i^\dagger]\} \\ \times \exp\{-\ln[\cosh(\kappa_0 t) \hat{a}^\dagger \hat{a}_s]\} \exp[-ie^{-i\theta} \tanh(\kappa_0 t) \hat{a}_i \hat{a}_s], \quad (3)$$

$$\hat{\rho}_{si, n_0} = N^2 \cosh^{-2(n_0+1)}(\kappa_0 t) \sum_{l, h} (-ie^{i\theta} \tanh \kappa_0 t)^l \\ \times (ie^{-i\theta} \tanh \kappa_0 t)^h \left[\begin{matrix} n_0+l \\ n_0 \end{matrix} \right] \left[\begin{matrix} n_0+h \\ n_0 \end{matrix} \right]^{1/2} |n_0+l\rangle_s |l\rangle_i \langle h|_s \langle n_0+h|, \quad (4)$$

$$\hat{\rho}_{si} = N'^2 e^{-|\alpha_0|^2} \sum_{k, l, h, n} \left[\begin{matrix} k+l \\ k \end{matrix} \right] \left[\begin{matrix} h+n \\ h \end{matrix} \right]^{1/2} \frac{(-ie^{i\theta} \tanh \kappa_0 t)^l (ie^{-i\theta} \tanh \kappa_0 t)^n}{\cosh^2 \kappa_0 t} \\ \times \left[\frac{\alpha_0}{\cosh \kappa_0 t} \right]^k \left[\frac{\alpha_0^*}{\cosh \kappa_0 t} \right]^h \frac{1}{\sqrt{k!}} \frac{1}{\sqrt{h!}} |k+l\rangle_s |l\rangle_i \langle n|_s \langle h+n|, \quad (5)$$

where N and N' are normalization constants and

$$\left[\begin{matrix} k \\ m \end{matrix} \right] = \frac{k!}{(k-m)!m!}.$$

When we simply want to know the signal state after parametric amplification, the reduced density operator can be calculated. No measurement process is involved. The reduced density operator for a number-state input signal is calculated by taking the trace of (4) with respect to idler variables,¹²

$$\hat{\rho}_{s, n_0}^{(\text{red})} \equiv \text{Tr}_i \hat{\rho}_{si, n_0} = N^2 \left[\frac{1}{\cosh \kappa_0 t} \right]^{2(n_0+1)} \sum_l \tanh^{2l} \kappa_0 t \left[\begin{matrix} n_0+l \\ n_0 \end{matrix} \right] |n_0+l\rangle_s \langle n_0+l|. \quad (6)$$

The quasiprobability density ${}_s \langle \alpha | \hat{\rho}_{s, n_0}^{(\text{red})} | \alpha \rangle_s$ is schematically shown in Fig. 1 for $n_0=0$ and $n_0 \neq 0$. The reduced density operator for a coherent-state input signal is calculated by taking the trace of (5),¹²

$$\hat{\rho}_s^{(\text{red})} = N'^2 e^{-|\alpha_0|^2} \sum_{k, l, h} \left[\begin{matrix} k+l \\ k \end{matrix} \right] \left[\begin{matrix} h+l \\ h \end{matrix} \right]^{1/2} \frac{\tanh^{2l} \kappa_0 t}{\cosh^2 \kappa_0 t} \left[\frac{\alpha_0}{\cosh \kappa_0 t} \right]^k \left[\frac{\alpha_0^*}{\cosh \kappa_0 t} \right]^h \frac{1}{\sqrt{k!}} \frac{1}{\sqrt{h!}} |k+l\rangle_s \langle h+l|. \quad (7)$$

The quasiprobability density ${}_s \langle \alpha | \hat{\rho}_s^{(\text{red})} | \alpha \rangle_s$ is schematically shown in Fig. 2.

III. STATE REDUCTION BY MEASUREMENT OF IDLER QUADRATURE AMPLITUDE

In this section and Sec. IV and Appendix A, we discuss the effect of idler output measurement on signal output. The conditional density operator is calculated by the well-defined generalized projection^{6,7} (operator-valued measure).

A measurement of idler quadrature amplitude with readout α'_1 is described by

$$|\alpha'_1\rangle_i \langle \alpha'_1|. \quad (8)$$

Since α_1 is defined over all real values of α_1 , $|\alpha_1\rangle_i \langle \alpha_1|$ means continuous projection. The operation-valued measure is introduced and removes the difficulty in the continuous spectrum.¹⁴ The density operator of a signal wave after readout α'_1 is

$$\hat{\rho}_s^{(\text{meas}, \alpha'_1)} \equiv \text{Tr}_i \hat{\rho}_i^{(\text{read}, \alpha'_1)} \hat{\rho}_{si} \\ = N'^2 \sum_{k, l, h, m} \frac{1}{\sqrt{m!} l!} \left[\frac{2}{\pi} \right]^{1/2} \exp(-2\alpha_1'^2) \frac{H_m(\sqrt{2}\alpha_1')}{2^{m/2}} \frac{H_l(\sqrt{2}\alpha_1')}{2^{l/2}} \exp(-|\alpha|^2) \left[\begin{matrix} h+m \\ h \end{matrix} \right] \left[\begin{matrix} k+l \\ k \end{matrix} \right]^{1/2} \\ \times \frac{[-i \tanh(\kappa_0 t) e^{+i\theta}]^l [i \tanh(\kappa_0 t) e^{-i\theta}]^m}{\cosh^2 \kappa_0 t} \frac{\alpha_A^k}{\sqrt{k!}} \frac{\alpha_A^{*h}}{\sqrt{h!}} |k+l\rangle_s \langle h+m|, \quad (9)$$

where a coherent-state input signal is assumed and

$$\hat{\rho}_i^{(\text{read}, \alpha'_1)} = \mathbf{1}_s \otimes |\alpha'_1\rangle_i \langle \alpha'_1| \quad (10)$$

In deriving (9), we used the following equation:⁵

$$\langle m | \alpha'_1 \rangle = \frac{1}{\sqrt{m!}} \left[\frac{2}{\pi} \right]^{1/4} \exp(-\alpha'^2_1) \frac{H_m(\sqrt{2}\alpha'_1)}{2^{m/2}} \quad (11)$$

Next the quasiprobability density of the conditional density operator is calculated. Without loss of generality, we assume $\theta = \pi/2$. Then the quasiprobability density is

$$\begin{aligned} Q^{(\text{meas}, \alpha'_1)}(\alpha) &\equiv_s \langle \alpha | \hat{\rho}_s^{(\text{meas}, \alpha'_1)} | \alpha \rangle_s \\ &= N_Q \exp[-(1 + \tanh^2 \kappa_0 t)(\alpha_1 - \langle \alpha_1 \rangle)^2] \exp \left[-\frac{1}{\cosh^2 \kappa_0 t} (\alpha_2 - \langle \alpha_2 \rangle)^2 \right], \end{aligned} \quad (12)$$

where

$$\begin{aligned} N_Q &= \left[\frac{1 + \tanh^2(\kappa_0 t)}{\pi} \right]^{1/2} \left[\frac{1}{\pi \cosh^2(\kappa_0 t)} \right]^{1/2}, \\ \langle \alpha_1 \rangle &= \frac{2 \tanh(\kappa_0 t) \alpha'_1 + \frac{\alpha_{0,1}}{\cosh(\kappa_0 t)}}{1 + \tanh^2(\kappa_0 t)}, \\ \langle \alpha_2 \rangle &= \alpha_{0,2} \cosh(\kappa_0 t). \end{aligned}$$

The quasiprobability density is Gaussian, centered at $\langle \alpha_1 \rangle$ and $\langle \alpha_2 \rangle$. The dispersion of the quadrature amplitudes can be calculated by using (12) as

$$\langle \Delta \alpha_1^2 \rangle = \langle \Delta \alpha_1^2 \rangle_Q - \frac{1}{4} = \frac{1}{4 \cosh(2\kappa_0 t)}, \quad (13)$$

$$\langle \Delta \alpha_2^2 \rangle = \langle \Delta \alpha_2^2 \rangle_Q - \frac{1}{4} = \frac{\cosh(2\kappa_0 t)}{4}. \quad (14)$$

Here $\langle \Delta \alpha_1^2 \rangle_Q$ and $\langle \Delta \alpha_2^2 \rangle_Q$ are the variances of the quasiprobability density (12) that are larger by $\frac{1}{4}$ than the intrinsic variances or $\hat{\rho}_s^{(\text{meas}, \alpha'_1)}$. The output-signal wave is reduced to a quadrature-amplitude squeezed state satisfying the minimum uncertainty product

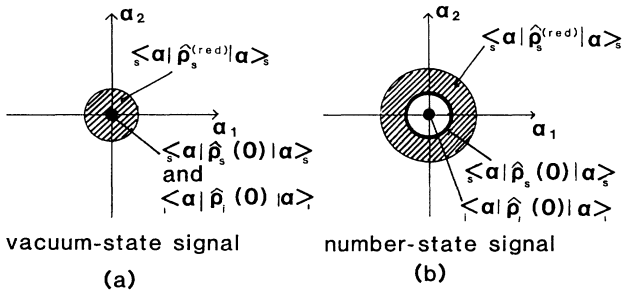


FIG. 1. (a) Quasiprobability densities of the initial density operators $\hat{\rho}_s(0) = |0\rangle_s \langle 0|$ and $\hat{\rho}_i(0) = |0\rangle_i \langle 0|$ and the reduced density operator $\hat{\rho}_s^{(\text{read})}$. (b) Quasiprobability densities of the initial density operators $\hat{\rho}_s(0) = |n_0\rangle_s \langle n_0|$, $\hat{\rho}_i(0) = |0\rangle_i \langle 0|$ and the reduced density operator $\hat{\rho}_s^{(\text{read})}$.

$$\langle \Delta \alpha_1^2 \rangle \langle \Delta \alpha_2^2 \rangle = \frac{1}{16}. \quad (15)$$

The quasiprobability density $\langle \alpha | \hat{\rho}_s^{(\text{meas}, \alpha'_1)} | \alpha \rangle_s$ is compared with that of the reduced density operator in Fig. 3.

IV. STATE REDUCTION BY A MEASUREMENT OF TWO IDLER QUADRATURE AMPLITUDES

A simultaneous measurement of two-quadrature amplitudes is described by the operation-valued measure

$$|\alpha'\rangle_i \langle \alpha'| \quad (16)$$

This corresponds to approximate simultaneous measurement.⁴ Following the idea of operation-valued measure,⁶ measurement of α_i by heterodynamic involves the product spaces $|\alpha_i\rangle_1 |0\rangle_2$, where 1 stands for the idler band and 2 stands for the image band that is in a vacuum state. Measurement of $|\alpha_i\rangle$ couples unavoidably to the zero-point fluctuations of the image band. Thus a measurement of $|\alpha_i\rangle$ must be interpreted as taking a trace of the product density matrix

$$\hat{\rho}_1 \otimes |0\rangle_2 \langle 0|,$$

i.e., forming the expression

$$\text{Tr}_1(\hat{\rho}_1 \otimes |0\rangle_2 \langle 0| \alpha)_{11} \langle \alpha|. \quad (17)$$

The conditional density operator after the readout α' is

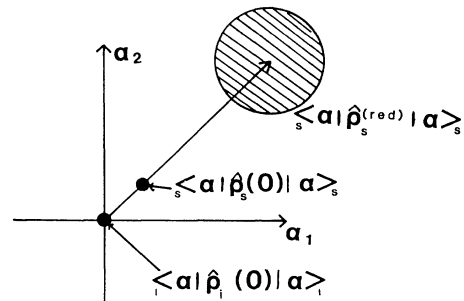


FIG. 2. Quasiprobability densities of the initial density operators $\hat{\rho}_s(0) = |\alpha_0\rangle_s \langle \alpha_0|$ and $\hat{\rho}_i(0) = |0\rangle_i \langle 0|$ and the reduced density operator $\hat{\rho}_s^{(\text{read})}$.

$$\begin{aligned}
\hat{\rho}_s^{(\text{meas}, \alpha')} &\equiv \text{Tr}_i \hat{\rho}_i^{(\text{read}, \alpha')} \hat{\rho}_{si} \\
&= N'^2 \sum_{k, h, l, n} \exp(-|\alpha'|^2) \exp(-|\alpha|^2) \frac{\alpha'^n}{\sqrt{n!}} \frac{\alpha'^l}{\sqrt{l!}} \left[\begin{matrix} h+n \\ h \end{matrix} \right] \left[\begin{matrix} k+l \\ k \end{matrix} \right]^{1/2} \frac{[-i \tanh(\kappa_0 t) e^{i\theta}]^l [i \tanh(\kappa_0 t) e^{-i\theta}]^n}{\cosh^2(\kappa_0 t)} \\
&\quad \times \frac{\alpha_A^k}{\sqrt{k!}} \frac{\alpha_A^{*h}}{\sqrt{h!}} |k+l\rangle_s \langle h+n|. \quad (18)
\end{aligned}$$

Here

$$\hat{\rho}_i^{(\text{read}, \alpha')} = \mathbf{1}_s \otimes |\alpha'\rangle_i \langle \alpha'|. \quad (19)$$

The quasiprobability density is

$$\begin{aligned}
Q^{(\text{meas}, \alpha')}(\alpha) &\equiv {}_s \langle \alpha | \hat{\rho}_s^{(\text{meas}, \alpha')} | \alpha \rangle_s \\
&= \frac{1}{\pi} \exp - |\alpha|^2 \\
&\quad - [i \tanh(\kappa_0 t) \alpha'^* e^{-i\theta} - \alpha_A]^2. \quad (20)
\end{aligned}$$

If $\theta = \pi/2$, the quasiprobability density is circular centered at $\langle \alpha_1 \rangle = \tanh(\kappa_0 t) \alpha'_1 + \alpha_{0,1} / \cosh(\kappa_0 t)$, $\langle \alpha_2 \rangle = -\tanh(\kappa_0 t) \alpha'_2 + \alpha_{0,2} / \cosh(\kappa_0 t)$. If the difference between the real dispersion and the dispersion of the quasiprobability density is taken into account, the output signal is reduced to a coherent state,

$$\langle \Delta \alpha_1^2 \rangle = \frac{1}{4},$$

and

$$\langle \Delta \alpha_2^2 \rangle = \frac{1}{4}. \quad (21)$$

The quasiprobability density ${}_s \langle \alpha | \hat{\rho}_s^{(\text{meas}, \alpha')} | \alpha \rangle_s$ is compared with that of the reduced density operator in Fig. 4.

V. PROJECTION OPERATORS GENERATING A NUMBER-PHASE SQUEEZED STATE, QUADRATURE-AMPLITUDE SQUEEZED STATE, AND COHERENT STATE

In Secs. III and IV we have shown that a nondegenerate parametric amplification process followed by a measurement produces various quantum light. Such a

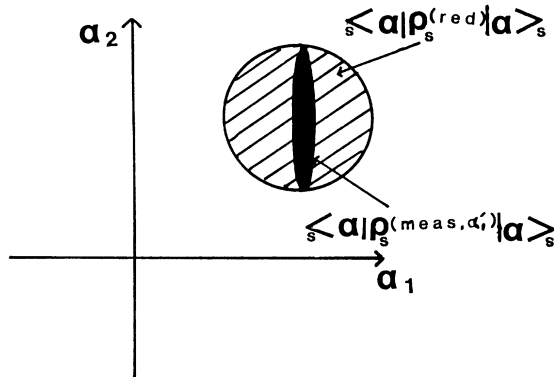


FIG. 3. Quasiprobability densities of the reduced density operator and conditional density operator for and idler wave quadrature-amplitude measurement. $\hat{\rho}_s(0) = |\alpha_0\rangle_s \langle \alpha_0|$.

quantum-light-generation process based on state reduction resulting from measurement is characterized by a projection operator¹⁵

$$\hat{P} = {}_p \langle \psi | \hat{U} | \phi \rangle_p. \quad (22)$$

Here $|\phi\rangle_p$ and $|\psi\rangle_p$ are the initial (prepared) state and final (measured) state of the probe system and \hat{U} is the evolution operator.

The projection operator $\hat{P}^{(m)}$ that characterizes an idler photon-number measurement scheme is written as

$$\begin{aligned}
\hat{P}^{(m)} &\equiv {}_i \langle m | \hat{U} | 0 \rangle_i \\
&= \frac{1}{\cosh(\kappa_0 t)} \frac{[-ie^{i\theta} \tanh(\kappa_0 t)]^m}{\sqrt{m!}} \hat{a}_s^{\dagger m} \\
&\quad \times \exp\{-\ln[\cosh(\kappa_0 t) \hat{a}_s^\dagger \hat{a}_s]\}. \quad (23)
\end{aligned}$$

This projection operator generates a number state $|n_0 + m\rangle_s$ from a number state $|n_0\rangle_s$. It also generates a number-phase squeezed state (41) in Appendix A from a coherent state $|\alpha_0\rangle_s$ (Ref. 11) (see also Appendixes A, B, and C).

The projection operator $\hat{P}^{(\alpha'_1)}$ that characterizes an idler quadrature-amplitude measurement scheme is given by

$$\begin{aligned}
\hat{P}^{(\alpha'_1)} &\equiv {}_i \langle \alpha'_1 | \hat{U} | 0 \rangle_i \\
&= N'' e^{-\alpha_1'^2} \exp \left[-2i \alpha_1' \tanh(\kappa_0 t) e^{i\theta} \hat{a}_s^\dagger \right. \\
&\quad \left. + \frac{\tanh^2(\kappa_0 t) e^{2i\theta}}{2} \hat{a}_s^{\dagger 2} \right] \\
&\quad \times \exp[-\ln(\cosh \kappa_0 t) \hat{a}_s^\dagger \hat{a}_s]. \quad (24)
\end{aligned}$$

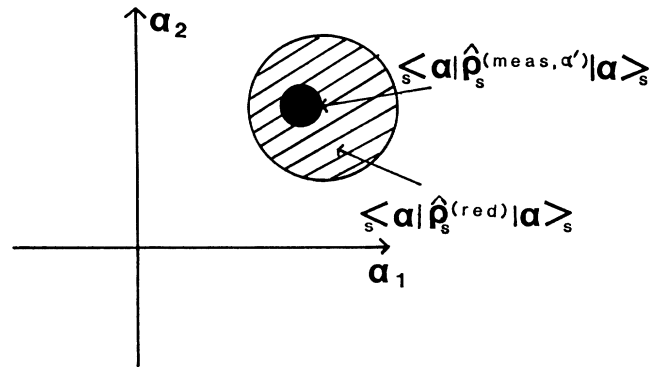


FIG. 4. Quasiprobability densities of the reduced density operator and conditional density operator for a measurement of the two idler wave quadrature amplitudes. $\hat{\rho}_s(0) = |\alpha_0\rangle_s \langle \alpha_0|$.

Here $N'' = [1/\cosh(\kappa_0 t)](2/\pi)^{1/4}$. This projection operator generates a quadrature-amplitude squeezed state (9) from a coherent state $|\alpha_0\rangle_s$.

The projection operator $\hat{P}^{(\alpha')}$ that characterizes a simultaneous-measurement scheme of the two idler quadrature amplitude is written as

$$\begin{aligned} \hat{P}^{(\alpha')} &\equiv_i \langle \alpha' | \hat{U} | 0 \rangle_i \\ &= \frac{e^{-|\alpha|^2/2}}{\cosh(\kappa_0 t)} \exp[-\alpha'^* \tanh(\kappa_0 t) e^{i\theta} \hat{a}_s^\dagger] \\ &\quad \times \exp\{-\ln[\cosh(\kappa_0 t) \hat{a}_s^\dagger \hat{a}_s]\}. \end{aligned} \quad (25)$$

This projection operator generates a coherent state (18) from a coherent state $|\alpha_0\rangle_s$.

VI. FEEDFORWARD

Even though an output signal wave is reduced to a number-phase squeezed state or quadrature-amplitude squeezed state for a specific readout m or α'_1 as demonstrated above, it is not considered to be a practical quantum-light-generation scheme. This is because each measurement produces a different readout and, if we want to know the quantum-statistical properties of all samples over all possible readouts, it is nothing but a signal-reduced density operator, as shown in Fig. 5.

In this section, we propose a method to overcome the preceding difficulty and produce a squeezed state continuously. Suppose a feedforward process operates on the output signal such that all the conditional density operators are translated to the same mean values $\langle \alpha_1 \rangle$ and $\langle \alpha_2 \rangle$ by using the measurement result as shown in Fig. 5. If the readout α''_1 is different from the most probable value α'_1 , then a translation operator

$$\hat{D}(\alpha''_1) = \exp[(\alpha'_1 - \alpha''_1)(\hat{a}_s^\dagger + \hat{a}_s)] \quad (26)$$

acts on the conditional density operator $\hat{\rho}_s^{(\text{meas}, \alpha'')}$. Then the result is

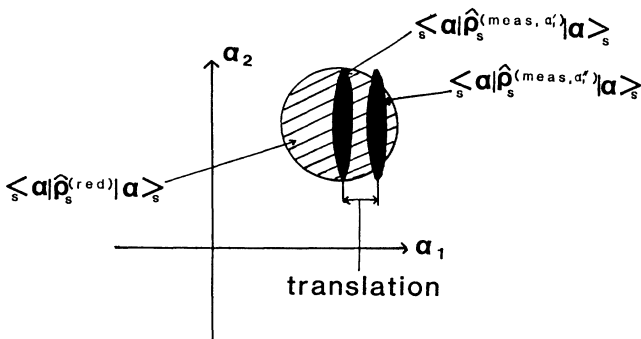


FIG. 5. Quasiprobability densities of the conditional density operator for different readouts α' and α'' . Unitary translation operator $D(\alpha'')$ maps $\hat{\rho}_s^{(\text{meas}, \alpha'')}$ onto $\hat{\rho}_s^{(\text{meas}, \alpha'_1)}$.

$$\begin{aligned} &_s \langle \alpha | \hat{D}(\alpha''_1) \hat{\rho}_s^{(\text{meas}, \alpha'')} \hat{D}^\dagger(\alpha''_1) | \alpha \rangle_s \\ &= \left[\frac{1 + \tanh^2(\kappa_0 t)}{\pi} \right]^{1/2} \left[\frac{1}{\pi \cosh^2(\kappa_0 t)} \right]^{1/2} \\ &\quad \times \exp\{-[1 + \tanh^2(\kappa_0 t)](\alpha_1 - \langle \alpha_1 \rangle)^2\} \\ &\quad \times \exp\left[-\frac{1}{\cosh^2(\kappa_0 t)}(\alpha_2 - \langle \alpha_2 \rangle)^2\right]. \end{aligned} \quad (27)$$

It is seen from (27) that a signal wave is always reduced to the same quadrature-amplitude squeezed state irrespective of the readout α''_1 . The translation operator $D(\alpha''_1)$ is practically realized by a phase modulator.¹⁰

VII. QUANTUM CORRELATION OF PHOTON TWINS EXPRESSED BY A HEISENBERG PICTURE

In this section we study the quantum correlation of photon twins in a Heisenberg picture and will come to the same conclusions we have previously obtained using a Schrödinger picture. If phase angle is appropriately selected, the input-output operators in a Heisenberg picture are described by

$$\hat{b}_s = \cosh(\kappa_0 t) \hat{a}_s + \sinh(\kappa_0 t) \hat{a}_i^\dagger, \quad (28)$$

and

$$\hat{b}_i^\dagger = \sinh(\kappa_0 t) \hat{a}_s + \cosh(\kappa_0 t) \hat{a}_i^\dagger. \quad (29)$$

From (28) and (29), and taking account of the commutation relation $[\hat{a}_s, \hat{a}_i^\dagger] = 0$, the difference between the signal photon number and probe photon number satisfies the following Manley-Rowe operator relation:

$$\hat{m}_s - \hat{m}_p = \hat{n}_s - \hat{n}_p. \quad (30)$$

Here $\hat{m}_s = \hat{b}_s^\dagger \hat{b}_s$, $\hat{m}_p = \hat{b}_i^\dagger \hat{b}_i$, $\hat{n}_s = \hat{a}_s^\dagger \hat{a}_s$, and $\hat{n}_p = \hat{a}_i^\dagger \hat{a}_i$. The dispersion difference between the signal and probe photon number is

$$\begin{aligned} \langle \Delta(\hat{m}_s - \hat{m}_p)^2 \rangle &= \langle \Delta(\hat{n}_s - \hat{n}_p)^2 \rangle \\ &= \begin{cases} 0 & (\text{number-state input}) \\ |\alpha_0|^2 & (\text{coherent-state input}) \end{cases}. \end{aligned} \quad (31)$$

Here we use the fact that the number dispersion of the input idler wave in a vacuum state is zero.

The complete photon-number correlation for an input signal in a number state corresponds to the result of (40). When an input signal is in a coherent state, on the other hand, the photon-number correlation is partly degraded by the photon-number variance $\langle \Delta \hat{n}_s^2 \rangle = |\alpha_0|^2$ of an input signal. At first sight this result seems to contradict the conclusion of (47) in Appendix A. But notice that (47) represents a dispersion in photon number for a readout m close to the most provable value $|\alpha_0|^2 \cosh^2 \kappa_0 t$ and that (31) represents the ensemble average of the photon-number correlation for all possible m_i values. In fact, the dispersion in photon number for a readout m much smaller than $|\alpha_0|^2 \cosh \kappa_0 t$ is reduced to zero, and that for a readout m much greater than $|\alpha_0|^2 \cosh \kappa_0 t$ is greater than $|\alpha_0|^2$. When these

different dispersions are integrated over all possible readout values with a proper probability density, we find a dispersion of not $|\alpha_0|^2/2$, but $|\alpha_0|^2$ (see Appendix D).

From (28) and (29), the output in-phase and phase-quadrature operators are related to the input operators by

$$\hat{b}_{s,1} = \cosh(\kappa_0 t) \hat{a}_{s,1} + \sinh(\kappa_0 t) \hat{a}_{i,1}, \quad (32)$$

$$\hat{b}_{i,1} = \sinh(\kappa_0 t) \hat{a}_{s,1} + \cosh(\kappa_0 t) \hat{a}_{i,1}. \quad (33)$$

The difference of output in-phase operators is

$$\hat{b}_{s,1} - \hat{b}_{i,1} = \exp(-\kappa_0 t) (\hat{a}_{s,1} - \hat{a}_{i,1}), \quad (34)$$

therefore its dispersion is

$$\langle \Delta(\hat{b}_{s,1} - \hat{b}_{i,1})^2 \rangle = \frac{1}{2} \exp(-2\kappa_0 t). \quad (35)$$

This result corresponds to the squeezed quadrature-amplitude noise (13). On the other hand, the quadrature component dispersion itself is

$$\langle \Delta \hat{b}_{s,2}^2 \rangle = \frac{1}{8} [\exp(-2\kappa_0 t) + \exp(2\kappa_0 t)]. \quad (36)$$

This corresponds to the enhanced quadrature-amplitude noise (14).

The dispersion of the sum of quadrature phase operators is similarly calculated as

$$\langle \Delta(\hat{b}_{s,2} + \hat{b}_{i,2})^2 \rangle = \frac{1}{2} \exp(-2\kappa_0 t). \quad (37)$$

They feature equally strong negative correlation.

VIII. CONCLUSION

Photon twins (signal and idler waves) produced by a high-gain parametric amplifiers feature strong positive correlation for both their photon numbers and in-phase amplitudes, and equally strong negative correlation for their phases and quadrature-phase amplitudes. If the

idler photon number, the single-quadrature amplitude, and the two-quadrature amplitudes are measured by a photon counter, homodyne detector, and heterodyne detector, the signal wave is reduced to a number-phase squeezed state, quadrature-amplitude squeezed state, and coherent state, respectively. The projection operators characterizing these nonunitary processes are given. With a feedforward technique, these can be used to generate various quantum lights.

ACKNOWLEDGMENTS

The authors would like to thank Professor Hermann, A. Haus, Dr. Nobuyuki Imoto, and Dr. Masahiro Kitagawa for useful discussion.

APPENDIX A

We discuss the effect of a photon-number measurement of idler output on signal output. A measurement of idler photon number with count m is described by the projection operator

$$|m\rangle_i \langle m|. \quad (38)$$

The density operator of a signal wave after the readout is calculated by

$$\hat{\rho}_s^{(\text{meas}, m)} \equiv \text{Tr}_i \hat{\rho}_i^{(\text{read}, m)} \hat{\rho}_{si}, \quad (39)$$

where $\hat{\rho}_i^{(\text{read}, m)} = \mathbf{1}_s \otimes |m\rangle_i \langle m|$ and $\mathbf{1}_s$ is an identity operator for a single wave.

For a number state input case, we obtain

$$\hat{\rho}_s^{(\text{meas}, m)} = |n_0 + m\rangle_s \langle n_0 + m|. \quad (40)$$

From (4) the output signal wave is also in a number state translated from the initial value n_0 by the exact number of readout m .

For coherent-state input, we get the following from (5):¹²

$$\begin{aligned} \hat{\rho}_s^{(\text{meas}, m)} = & N'^2 \sum_{k,h} \exp(-|\alpha_0|^2) \left[\begin{matrix} h+m \\ h \end{matrix} \right] \left[\begin{matrix} k+m \\ k \end{matrix} \right]^{1/2} \frac{\tanh^{2m}(\kappa_0 t)}{\cosh^2(\kappa_0 t)} \\ & \times \left[\frac{\alpha_0}{\cosh(\kappa_0 t)} \right]^k \left[\frac{\alpha_0^*}{\cosh(\kappa_0 t)} \right]^h \left[\frac{1}{h!k!} \right]^{1/2} |k+m\rangle_s \langle h+m|. \end{aligned} \quad (41)$$

The photon-number probability density function is calculated as

$$\begin{aligned} P(n) \equiv & \langle n | \hat{\rho}_s^{(\text{meas}, m)} | n \rangle_s \\ = & \frac{1}{F(1+m, 1; N_A)} \binom{n}{n-m} N_A^{n-m} \frac{1}{(n-m)!}, \end{aligned} \quad (42)$$

where $N_A = |\alpha_0|^2 / \cosh^2(\kappa_0 t)$ and $F(a, b; c)$ is Kummer function given by

$$F(a, b; c) = \frac{\Gamma(1+a)}{\Gamma(1+b)} \sum_j \frac{\Gamma(1+a+j)c^j}{\Gamma(1+b+j)j!}. \quad (43)$$

The average photon number and its dispersion is ob-

tained using the probability $P(n)$ as

$$\langle n \rangle \equiv \sum_{j>m} j P(j) = (m+1) \frac{L_{m+1}(-N_A)}{L_m(-N_A)} - 1, \quad (44)$$

$$\begin{aligned} \langle \Delta n^2 \rangle \equiv & \sum_{j>m} (j - \langle j \rangle)^2 P(j) \\ = & (m+2)(m+1) \frac{L_{m+2}(-N_A)}{L_m(-N_A)} \\ & - (m+1)^2 \left[\frac{L_{m+1}(-N_A)}{L_m(-N_A)} \right]^2 \\ & - (m+1) \frac{L_{m+1}(-N_A)}{L_m(-N_A)}. \end{aligned} \quad (45)$$

Derivation of (45) used the relation

$$F(1+m, 1; N_A) = L_m(-N_A) \exp(N_A),$$

where $L_m(x)$ is a Laguerre polynomial. When the parametric-amplifier gain is high enough, $\kappa_0 t \gg 1$, and the readout m is in the vicinity of the most probable value, $m \sim |\alpha_0|^2 \cosh^2 \kappa_0 t$, the average photon number and its dispersion derived in Appendix B are approximately given by

$$\langle n \rangle \sim m + |\alpha_0|^2, \quad (46)$$

and

$$\begin{aligned} P(\cos\psi) &= {}_s \langle \cos\psi | \hat{\rho}_s^{(\text{meas}, m)} | \cos\psi \rangle_s \\ &= \sum_{k,h} \frac{2}{\pi} \sin(k+m+1)\psi \sin(h+m+1)\psi \left[\begin{matrix} h+n \\ h \end{matrix} \right] \left[\begin{matrix} k+m \\ k \end{matrix} \right]^{1/2} \frac{\alpha_A^k}{\sqrt{k!}} \frac{\alpha_A^{*h}}{\sqrt{h!}}, \quad (48) \\ P(\sin\psi) &\equiv {}_s \langle \sin\psi | \hat{\rho}_s^{(\text{meas}, m)} | \sin\psi \rangle_s \\ &= \sum_{k,h} \frac{1}{2\pi} [e^{i(k+m+1)\psi} - e^{-i(k+m+1)(\psi-\pi)}] [e^{i(h+m+1)\psi} - e^{-i(h+m+1)(\psi-\pi)}] \\ &\quad \times \left[\begin{matrix} h+m \\ h \end{matrix} \right] \left[\begin{matrix} k+m \\ k \end{matrix} \right]^{1/2} \frac{\alpha_A^k}{\sqrt{k!}} \frac{\alpha_A^{*h}}{\sqrt{h!}}, \quad (49) \end{aligned}$$

where $\alpha_A = \alpha_0 / \cos(\kappa_0 t)$. Straightforward calculation leads to

$$\begin{aligned} \langle \cos\psi \rangle &\equiv \int_0^\pi \cos\psi P(\cos\psi) d\psi \\ &= N_A^{1/2} [F(1+m, 1; N_A)]^{-1} \Psi_{1,m}(N_A) \cos\phi_{\alpha_0}, \quad (50) \end{aligned}$$

$$\begin{aligned} \langle \sin\psi \rangle &\equiv \int_{-\pi/2}^{\pi/2} \sin\psi P(\sin\psi) d\psi \\ &= N_A^{1/2} [F(1+m, 1; N_A)]^{-1} \Psi_{1,m}(N_A) \sin\phi_{\alpha_0}, \quad (51) \end{aligned}$$

$$\begin{aligned} \langle \cos^2\psi \rangle &\equiv \int_0^\pi \cos^2\psi P(\cos\psi) d\psi \\ &= \frac{1}{2} - \frac{\delta_{m,0}}{4} [F(1+m, 1; N_A)]^{-1} \\ &\quad + \frac{N_A}{2} [F(1+m, 1; N_A)]^{-1} \Psi_{2,m}(N_A) \\ &\quad \times \cos(2\phi_{\alpha_0}), \quad (52) \end{aligned}$$

$$\begin{aligned} \langle \sin^2\psi \rangle &\equiv \int_{-\pi/2}^{\pi/2} \sin^2\psi P(\sin\psi) d\psi \\ &= \frac{1}{2} - \frac{\delta_{m,0}}{4} [F(1+m, 1; N_A)]^{-1} \\ &\quad - \frac{N_A}{2} [F(1+m, 1; N_A)]^{-1} \Psi_{2,m}(N_A) \cos(2\phi_{\alpha_0}), \quad (53) \end{aligned}$$

$$\langle \Delta n^2 \rangle \sim \frac{|\alpha_0|^2}{2}. \quad (47)$$

Note that the input signal has the photon-number dispersion $\langle \Delta n(0)^2 \rangle = |\alpha_0|^2$. It is reduced by a factor of 2 after the parametric amplification and photon-counting measurement. This result was first discovered by Yuen¹⁶ and was later confirmed numerically by Kitagawa and Yamamoto.¹² Since m is much greater than $|\alpha_0|^2$ in a high-gain parametric amplifier, the signal wave features a strong sub-Poissonian distribution.

Next the phase dispersion is calculated. The sine and cosine probability density functions are calculated in a manner similar to the photon-number probability density function,

where $\phi_{\alpha_0} = \arctan \alpha_0$ and $\cos\phi_{\alpha_0}$ and $\sin\phi_{\alpha_0}$ are the average sine and cosine operator values of an input signal. $\delta_{i,j}$ is Kronecker's δ ,

$$\Psi_{1,m}(N_A) = \sum_k \frac{(k+m)!}{k!m!} \left[\frac{k+m+1}{k+1} \right]^{1/2} \frac{N_A^k}{k! \sqrt{k+1}} \quad (54)$$

and

$$\begin{aligned} \Psi_{2,m}(N_A) &= \sum_k \frac{(k+m)!}{k!m!} \left[\frac{(k+m+2)(k+m+1)}{(k+2)(k+1)} \right]^{1/2} \\ &\quad \times \frac{N_A^k}{k! \sqrt{(k+2)(k+1)}}. \quad (55) \end{aligned}$$

Note that $\Psi_{1,0}(N_A) = \Psi_1(N_A)$ and $\Psi_{2,0}(N_A) = \Psi_2(N_A)$, where $\Psi_1(N_A)$ and $\Psi_2(N_A)$ are shown in Ref. 17.

When the parametric-amplifier gain is high enough, $\kappa_0 t \gg 1$, and the readout m is in the vicinity of the most probable value,

$$m \sim |\alpha_0|^2 \cosh^2(\kappa_0 t),$$

the average sine and cosine operator values and the normalized dispersion are approximately calculated (see Appendix C) as

$$\langle \cos\psi \rangle \sim \left[1 - \frac{1}{4|\alpha_0|^2} \right] \cos\phi_{\alpha_0}, \quad (56)$$

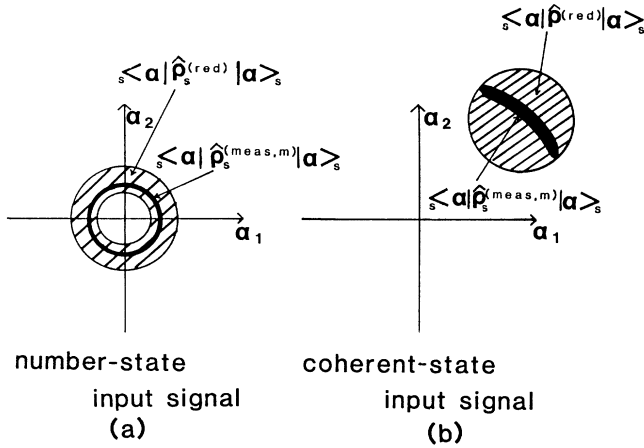


FIG. 6. Quasiprobability densities of the reduced density operator and conditional density operator for an idler photon-number measurement. (a) $\hat{\rho}_s(0) = |n_0\rangle_s \langle n_0|$ and (b) $\hat{\rho}_s(0) = |\alpha_0\rangle_s \langle \alpha_0|$.

$$\langle \sin \psi \rangle \sim \left[1 - \frac{1}{4|\alpha_0|^2} \right] \sin \phi_{\alpha_0}, \quad (57)$$

and

$$\frac{\langle \Delta \sin^2 \psi \rangle}{\langle \cos \psi \rangle} \sim \frac{1}{2|\alpha_0|^2}. \quad (58)$$

Note that the normalized sine operator dispersion of an input-signal wave is $1/4|\alpha_0|^2$. It is enhanced by a factor of 2 after parametric amplification. This doubling of quantum noise is a manifestation of a general quantum limit of linear amplifiers and simultaneous measurement of the two conjugate observables.¹⁸

From (47) and (58) we see that the signal wave after measurement of idler photon number is reduced to a number-phase squeezed state, satisfying the minimum uncertainty product of photon number and sine operators,

$$\frac{\langle \Delta n^2 \rangle \langle \Delta \sin^2 \psi \rangle}{\langle \cos \psi \rangle^2} \sim \frac{1}{4}. \quad (59)$$

The quasiprobability density ${}_s \langle \alpha | \hat{\rho}_s^{(meas,m)} | \alpha \rangle_s$ of thus generated number states and number-phase squeezed states are compared with those for the reduced density operator in Fig. 6.

APPENDIX B

We derive the approximate value of photon-number dispersion (47). Suppose the readout m of the output idler photon number is in the vicinity of the most probable, $|\alpha_0|^2 \cosh^2 \kappa_0 t$. The relations

$$L_m(-z) = e^{-z} F(1+m, 1; z) \quad (60)$$

and

$$F(a+1, b; x) = F(a, b; x) + \frac{x}{b} F(a+1, b+1; x) \quad (61)$$

from (45) give us

$$\begin{aligned} \langle \Delta n^2 \rangle &= 2(m+2)(m+1)z \frac{F(m+2, 2, z)}{F(m+1, 1, z)} \\ &+ (m+2)(m+1) \frac{z^2}{2} \frac{F(m+3, 3, z)}{F(m+1, 1, z)} \\ &- (m+1)^2 z^2 \left[\frac{F(m+2, 2, z)}{F(m+1, 1, z)} \right]^2 \\ &- 2(m+1)^2 z \frac{F(m+2, 2, z)}{F(m+1, 1, z)} \\ &- (m+1)z \frac{F(m+2, 2, z)}{F(m+1, 1, z)}, \end{aligned} \quad (62)$$

where $z = |\alpha_0|^2 / \cosh(\kappa_0 t)$. Further applying the relations,

$$F\left[a, c; \frac{x}{a}\right] \rightarrow \Gamma(c) x^{(1-c)/2} I_{c-1}(2\sqrt{x}) \quad \text{as } a \rightarrow \infty \quad (63)$$

and

$$I_{c+1}(x) = I_{c-1}(x) - \frac{2c}{x} I_c(x), \quad (64)$$

and taking the limit as $z \rightarrow 0$ and $zm \rightarrow z_0$, we obtain

$$\langle \Delta n^2 \rangle \rightarrow z_0 \left[1 - \left[\frac{I_1(2\sqrt{z})}{I_0(2\sqrt{z})} \right]^2 \right], \quad (65)$$

where $\Gamma(x)$ is the γ function and $I_k(x)$ is the modified Bessel function.

If the input average photon number is much greater than one, $z_0 \gg 1$,

$$I_0(2\sqrt{z_0}) = e^{2\sqrt{z_0}} F\left(\frac{1}{2}, 1, -4\sqrt{z_0}\right). \quad (66)$$

By using (66) and the expansion

$$F(a, b, -x) \sim x^{-a} \frac{\Gamma(b)}{\Gamma(b-a)} [1 + a(1+a-b)] x^{-1} \quad (67)$$

in (65), we obtain

$$\frac{I_1(2\sqrt{z})}{I_0(2\sqrt{z})} \sim 1 - \frac{1}{4} z_0^{-1/2} \quad (68)$$

and

$$\langle \Delta n^2 \rangle \sim \frac{1}{2} z_0^{1/2} \sim \frac{1}{2} |\alpha_0|^2. \quad (69)$$

APPENDIX C

We derive the normalized sine dispersion (58). Equation (54) can be rewritten as

$$\Psi_{1,m}(z) = \frac{1}{m^{1/2}} \sum_k \frac{(k+m)!}{(k+1)!(m-n)!} \left[1 + \frac{k+1}{m} \right]^{1/2} \frac{z^k}{k!}. \quad (70)$$

Since m is sufficiently large, there is always an N_0 such that $k+1/m$ for $k < N_0$. Since the terms for $k > N_0$ do not contribute to the sum, we can set

$$\begin{aligned} \Psi_{1,m}(z) &\sim \frac{1}{m^{1/2}} \sum_k \frac{(k+m)!}{(k+1)!(m-1)!} \frac{z^k}{k!} \\ &= m^{1/2} F(1+m, 2; z). \end{aligned} \quad (71)$$

From (50), (51), and (63), we obtain

$$\begin{aligned} \langle \cos\psi \rangle &\sim \frac{I_1(2\sqrt{z_0})}{I_0(2\sqrt{z_0})} \cos\phi_{\alpha_0} \sim \left[1 - \frac{1}{4|\alpha_0|^2} \right] \cos\phi_{\alpha_0}, \\ \langle \sin\psi \rangle &\sim \frac{I_1(2\sqrt{z_0})}{I_0(2\sqrt{z_0})} \sin\phi_{\alpha_0} \sim \left[1 - \frac{1}{4|\alpha_0|^2} \right] \sin\phi_{\alpha_0}. \end{aligned} \tag{72}$$

By a similar approximation, we get

$$\begin{aligned} \Psi_{2,m}(z) &\sim \sum_k \frac{(k+m)!}{(k+2)!(m-1)!} \frac{z^k}{k!} \\ &= \frac{m}{2} F(1+m, 3; z) \\ &\sim mz_0^{-1} I_2(2\sqrt{z_0}). \end{aligned} \tag{73}$$

Here (63) was used. By (53), (63), and (73), we obtain

$$\langle \sin^2\psi \rangle \sim \frac{1}{2} \left[1 - \frac{I_2(2\sqrt{z_0})}{I_0(2\sqrt{z_0})} \cos 2\phi_{\alpha_0} \right]. \tag{74}$$

From (64) and (68), we get

$$\frac{\langle \sin^2\psi \rangle}{\langle \cos\psi \rangle^2} \sim \tan^2\phi_{\alpha_0} + \frac{1}{2}z_0^{-1/2}. \tag{75}$$

Since $|\langle \sin\psi \rangle / \langle \cos\psi \rangle|^2 \sim \tan^2\phi_{\alpha_0}$, the normalized sine uncertainty is given by

$$\frac{\langle \Delta \sin^2\psi \rangle}{\langle \cos\psi \rangle^2} \sim \frac{1}{2}z_0^{-1/2} \sim \frac{1}{2|\alpha_0|^2}. \tag{76}$$

APPENDIX D

We calculate $\langle \Delta(m_s - m_i)^2 \rangle$ using the Schrödinger picture. First we calculate $\langle m_s - m_i \rangle$. From (2), we obtain

$$\begin{aligned} \langle m_s - m_i \rangle &= \text{Tr}_{s,i} \hat{\rho}_{si} (\hat{n}_s \otimes \mathbf{1}_i - \mathbf{1}_s \otimes \hat{n}_i) = e^{-|\alpha_0|^2} \sum_i \frac{[\tanh^2(\kappa_0 t)]^i}{\cosh(\kappa_0 t)} \sum_j (j-1) \begin{bmatrix} j \\ j-i \end{bmatrix} \frac{z^{j-1}}{(j-i)!} \\ &= e^{-|\alpha_0|^2} \sum_i \frac{[\tanh^2(\kappa_0 t)]^i}{\cosh(\kappa_0 t)} z \frac{dF(1+i, 1; z)}{dz}. \end{aligned} \tag{77}$$

z is defined below (62). By using

$$\frac{dF(a, b; x)}{dx} = \frac{a}{b} F(a+1, b+1; x), \quad F(a, b; z) = e^z F(b-a, b, -z),$$

from (77) and

$$F(-a, 1+b, x) = \frac{\Gamma(b+1)\Gamma(a+1)}{\Gamma(b+a+1)} L_a^b(x), \tag{78}$$

we obtain

$$\langle m_s - m_i \rangle = \frac{ze^{-|\alpha_0|^2}}{\cosh^2 \kappa_0 t} \sum_i \tanh^{2i} \kappa_0 t L_i^1(-z) = |\alpha_0|^2. \tag{79}$$

In deriving last the equality of (79), we use

$$\sum_k L_k^a(z) x^k = (1-x)^{-a-1} e^{xz/(x-1)}. \tag{80}$$

Next we derive $\langle (m_s - m_i)^2 \rangle$ with a similar procedure,

$$\begin{aligned} \langle (m_s - m_i)^2 \rangle &= \text{Tr}_{s,i} \hat{\rho}_{si} (\hat{n}_s \otimes \mathbf{1}_i - \mathbf{1}_s \otimes \hat{n}_i)^2 \\ &= e^{-|\alpha_0|^2} \sum_i \frac{[\tanh^2(\kappa_0 t)]^i}{\cosh(\kappa_0 t)} \left[z^2 \frac{d^2 F(1+i, 1; z)}{dz^2} + z \frac{dF(1+i, 1; z)}{dz} \right] \\ &= |\alpha_0|^4 + |\alpha_0|^2. \end{aligned} \tag{81}$$

In deriving of last equality of (81), we use (78) and (79). Therefore we obtain

$$\langle \Delta(m_s - m_i)^2 \rangle = |\alpha_0|^2. \tag{82}$$

- ¹R. E. Slusher *et al.*, Phys. Rev. Lett. **55**, 2409 (1985).
²L. Wu, H. Kimble, J. Hall, and H. Wu, Phys. Rev. Lett. **57**, 2520 (1986).
³S. Machida, Y. Yamamoto, and Y. Itaya, Phys. Rev. Lett. **58**, 1000 (1987).
⁴E. Arthurs and J. L. Kelly, Jr., Bell System. Tech. J. **44**, 725 (1965).
⁵H. P. Yuen and J. H. Shapiro, IEEE Trans. Inf. Theory **IT26**, 78 (1980).
⁶C. W. Helstrom, Int. J. Theor. Phys. **8**, 361 (1973).
⁷E. B. Davies, *Quantum Theory of Open System* (Academic, New York, 1976).
⁸M. Kitagawa, N. Imoto, and Y. Yamamoto, Phys. Rev. A **35**, 5270 (1987).
⁹D. C. Burnham and D. L. Weinberg, Phys. Rev. Lett. **25**, 84 (1970).
¹⁰G. Björk and Y. Yamamoto, Phys. Rev. A **37**, 4229 (1988).
¹¹B. R. Mollow and R. J. Glauber, Phys. Rev. **160**, 1097 (1967).
¹²M. Kitagawa and Y. Yamamoto (unpublished).
¹³B. L. Schumaker and C. M. Caves, Phys. Rev. A **31**, 3093 (1985).
¹⁴E. B. Davies and J. T. Lewis, Commun. Math. Phys. **17**, 239 (1970).
¹⁵J. P. Gordon and W. H. Louisell, in *Physics of Quantum Electronics*, edited by P. L. Kelly *et al.* (McGraw-Hill, New York, 1968).
¹⁶H. P. Yuen, Phys. Rev. Lett. **56**, 2176 (1986).
¹⁷P. Carruthers and M. M. Nieto, Rev. Mod. Phys. **40**, 411 (1968).
¹⁸Y. Yamamoto and H. A. Hans, Rev. Mod. Phys. **58**, 1001 (1986).